

Article

Experimental Study on Flexural Behavior of TRM-Strengthened RC Beam: Various Types of Textile-Reinforced Mortar with Non-Impregnated Textile

Jongho Park ¹ , Sungnam Hong ² and Sun-Kyu Park ^{1,*}

¹ Department of Civil, Architectural and Environmental System Engineering, Sungkyunkwan University, Suwon 16419, Gyeonggi-do, Korea; rhapsode@skku.edu

² Department of Ocean Civil Engineering, Gyeongsang University, Tongyeong 53064, Gyeongsangnam-do, Korea; snhong@gnu.ac.kr

* Correspondence: skpark@skku.edu; Tel.: +82-031-290-7530

Received: 10 April 2019; Accepted: 9 May 2019; Published: 15 May 2019



Abstract: In this study, to compare strengthening efficiency and flexural behaviors of textile-reinforced mortar (TRM) according to various types of strengthening methods without the textile being impregnated, ten specimens were tested. The results showed that TRM was beneficial for uniform distribution of cracks and increased the strengthening efficiency and load-bearing capacity, as textile reinforcement ratio and textile lamination increased and the mesh size of the textile decreased and mechanical end anchorage applied. However, the strengthening effect was shown obviously until the yield load considering structural safety and serviceability.

Keywords: textile reinforced mortar; non-impregnated textile; textile reinforcement ratio; textile lamination; mesh size; end anchorage; strengthening efficiency

1. Introduction

Due to aging infrastructures, the need for improvement in repair, strengthening, and maintenance processes has been continuously increasing. To improve the performance of aging infrastructures, astronomical funds have been invested [1]. Moreover, with the development of design code, structures are required to be strengthened to meet structural safety [2]. To keep up with these requirements, fiber-reinforced polymer (FRP) strengthening method has been studied and applied for many years [3–5]. Strengthening with FRP uses organic materials such as epoxy resin for bonding with concrete substrate. However, organic materials have several disadvantages, including the impossibility of applying them to wet surfaces, low glass transition temperature, low fire resistance, and low permeability.

To overcome the disadvantages of the use of organic materials, textile-reinforced mortar (TRM) method using inorganic materials such as cementitious matrix has been actively researched recently [2,6–8]. TRM is a structure-strengthening method for attaching textiles composed of fiber materials, such as carbon and glass fibers with excellent chemical resistance, to the surface of masonry and reinforced concrete (RC) structures generally using mortar. As it uses mortar, TRM is highly resistant to temperatures and applicable to wet surfaces, thus allowing efficient construction in various environments. However, since the textile consists of numerous filaments, the mortar cannot penetrate into the textile and the bonding with mortar is divided into the inner and the outer.

Many researchers investigated the bonding behavior between textile and mortar and between TRM layer and concrete substrate to explain the bonding characteristics of textile composite materials [9–14]. Furthermore, to improve the bonding between textile and mortar, textile has been impregnated with

resin or attached small sand grains [15–20]. This reinforcement of textile enables its tensile strength to be used more efficiently.

Papanicolaou et al. [15] coated a textile using a polymeric resin. Compared with the uncoated specimens, the load of specimen reinforced with the textile alone was increased by 26–112% in terms of the first-crack, yield and ultimate load. The load of specimen reinforced with the textile and steel rebar increased by 11–16%. The effect of strengthening using coated textile was increased when reinforcing by textile alone, or when using a smaller amount of textile. Kamani et al. [19] applied a partially impregnated epoxy at the interaction point of weft and warp roving in textile. Experimental results show that the maximum load of specimens with partially impregnated epoxy was increased by 49–73%. In Raoof et al. [21], the flexural strength of the specimens with coated textile was increased by 16% at crack and by 5% at yield and ultimate load. The failure mode of specimens was changed from premature failure due to local slippage of uncoated textile to interlaminar shearing of mortar of coated textile. Jesse et al. [22] also showed that the ultimate load of the specimen with coated textile was increased by 23% compared with the uncoated specimen.

Commonly, impregnation or coating of textile improves the bond condition between textile and mortar. In addition, fiber alignment, prevention of relative slippage, strain compatibility of filaments, and the ease of load transferring due to strong binding of the intersection point of textile was studied [15,19]. The process of impregnation makes it possible to use the textile more efficiently, but the efficiency differs depending on the type of the resin and textile, impregnation method, and the shape of the structure. In addition, according to Gutierrez et al. [23], the additional cost of resin and impregnation process accounts for about 38% of the fiber in terms of raw materials.

Therefore, in this study, various types of TRM were investigated to solve the problem of cost due to textile impregnation and to find a method of using textile efficiently without the impregnation process. According to previous studies, the non-impregnated textile will cause the bond of textile and mortar to be divided into inner and outer filaments so that the tensile strength of TRM composite is decreased. Hence, to prevent the slippage and damage of textiles, various methods of textile lamination, textile geometry, and end anchorage were applied. Ten specimens were fabricated and compared with load and deflection relationship, cracking, strain, and ductility index to investigate the strengthening efficiency and flexural behavior of TRM without textile impregnation.

2. Experimental Program

2.1. Textile

The textile used in this study was made by alkali resistant (AR) glass fibers containing 16.5% zircon in 8×8 mm intervals as shown in Figure 1. Properties of the textiles provided by the manufacturer (Taishan fiberglass Inc., Tai'an, China) are listed in Table 1. The diameter of the filament was $14 \mu\text{m}$, and the area of roving was 0.246 mm^2 . Its tensile strength, modulus of elasticity, and maximum strain were 1789 MPa, 68 GPa, and 0.0262, respectively.



Figure 1. Alkali resistant (AR) glass textile.

Table 1. Detailed specifications of the AR glass provided by the manufacturer; AR: Alkali Resistant.

Properties and Geometric Parameters ¹	AR Glass
Number of filaments per roving	1600
Tensile strength of warp (N/50 mm)	2142
Tensile strength of weft (N/50 mm)	1833
Rupture elongation ratio of warp (%)	2.85
Rupture elongation ratio of weft (%)	2.36
Tex of yarn (g/km)	640
Diameter or filament (μm)	14

¹ Tested by Chinese standard: GB/T 7689.5 idt ISO 4606.

2.2. Matrix

Ready-mixed concrete with specified concrete strength up to 35 MPa was used. The average compressive strength of the concrete using three cylindrical specimens with a 100 mm diameter and a 200 mm height was 42.19 MPa. For the matrix of the TRM section, polymer mortar was used for effective bonding with the textile and concrete substrate. The concrete and polymer mortar mix proportions are listed in Tables 2 and 3. Specifications of polymer mortar provided by the manufacturer (SsangYong Cement, Seoul, South Korea) are listed in Table 4. The average compressive strength of the polymer mortar using three cylindrical specimens was 48.91 MPa.

Table 2. Mix proportions of concrete.

W/B (%)	Unit Weight (kg/m^3)						
	Cement	Water	Fine Aggregate	Coarse Aggregate	Fly Ash	Blast Furnace Slag	Water Reducer
35.8	319	163	780	898	68	68	4.1

Table 3. Mix proportions of polymer mortar.

W/M ¹ (%)	Content Per 1 Bag of 25 kg (%)					
	Cement	Fine Aggregate	PVA Fiber ²	Acrylate Copolymer	CSA ³	Water Reducer
19	<50	35~40	>1	3>	>5	<1

¹ Water/mortar. ² Polyvinyl alcohol fiber. ³ Expansive admixture.

Table 4. Detailed specifications of the polymer mortar provided by the manufacturer.

Strength Type	Experimental Value (MPa)	Standard of KS (MPa)
Flexural	8	6.0 >
Compressive	45	20.0 >
Bond ¹	1.5	1.0 >

¹ The bond strength is improved 20% with primer.

2.3. Specimen

Nine TRM-strengthened reinforced-concrete beams were fabricated as TRM specimens, and one RC beam was fabricated as a control specimen. TRM specimens are composed of the RC and TRM. Total length was 1500 mm, width was 120 mm, and height was 150 mm, which consist of a height of 135 mm of RC and a height of 15 mm of TRM. The control specimen had a height of 135 mm without TRM strengthening layer. RC was reinforced with two D10 bars with diameter 9.53 mm in tension. To prevent the shear failure at support section, D6 shear stirrups with diameter 6.35 mm were placed at 80 mm and 100 mm intervals except for the pure bending section. Yield strength and modulus

of elasticity of the reinforcement were 400 MPa and 200 GPa for rebar D6 and D10, respectively. Specifications of these study specimens are shown in Figure 2.

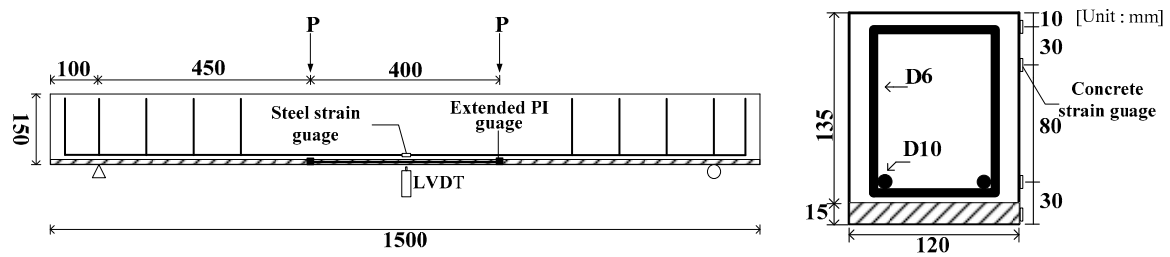


Figure 2. Specifications of study specimens.

Experimental parameters of the TRM specimen and the experimental comparison group were as follows: (1) Textile reinforcement ratio (RC, T1, T2, T3); (2) textile lamination and geometry (T1, T1O, T1N, T1M); and (3) end anchorage (T2, T2E, T2A, T2AP).

The procedures for preparing the TRM specimen were as follows: (1) Grinding the bottom surface of RC beam with grid of grooves with depth of 2–3 mm; (2) setting up a RC beam to a strengthening device; (3) applying a primer; (4) pouring polymer mortar with thickness of 4 mm by using a trowel; (5) fixing the first textile on the clamp device at each side as shown in Figure 3; (6) stretching the textile to parallel to reinforcing axis; (7) pouring second polymer mortar with thickness of 2–3 mm and applying hand pressure to penetrate mortar into the textile; (8) repeat step (5)–(7) until all designed textile layers were placed; (9) after last textile was placed, mortar poured with 4 mm thickness. The average thickness of the TRM strengthening layer of all specimens was 19.91 mm, which was larger than the design as shown in Figure 2. This is because the amount of mortar required for TRM was increased due to the grooves 2–3 mm deep and the thicker textile layer due to lamination. Detailed specifications of these study specimens are listed in Table 5.



Figure 3. Textile-reinforced mortar (TRM)-strengthening device with textile stretching.

Table 5. Detailed specifications of study specimens.

Name	Strengthening Configuration	Textile		End Anchorage
		Layer	Lamination ²	
Control	Reinforced concrete	-	-	-
T1 ¹	Textile reinforcement ratio was 0.049%	3	-	×
T1N	Textile applied manually (non-stretching)	3	-	×
T1O	Three textiles lamination in one layer	1	3	×
T1M ²	Textile mesh size changed from 8 mm to 24 mm	3	(1/3) × 3	×
T2 ¹	Textile reinforcement ratio was 0.098%	3	2	×
T2E ³	Fixed to both ends of the beam by TRM	3	2	○
T2A ³	L-shaped angle + bolt anchor	3	2	○
T2AP ³	Steel plate + bolt anchor	3	2	○
T3 ¹	Textile reinforcement ratio was 0.15%	3	3	×

¹ A reference specimen for each experimental group. ² The number of roving T1M per one layer was reduced to one third due to changed mesh size. ³ TRM specimens were applied with end anchorage.

T denotes the beam reinforced with TRM, and the number denotes the ratio of textile reinforcement. Textile reinforcement ratio of T1 was 0.049% (8.86 mm²). T2 and T3 were two and three times that of T1, respectively. T1N applied textile manually without textile stretching. All specimens except T1N were fabricated using a TRM-strengthening device as shown in Figure 3, which was fixing textiles on both sides of the specimen to keep the textile parallel to reinforcing axis when mortar pouring [24]. Textile stretching was applied with a slight tension so as not to damage the fibers [17–19]. T1O was laminated with three textiles to one layer. The mesh size of T1M was changed from 8 mm to 24 mm. T2E was fixed to both ends of the beam by TRM. T2A and T2AP were applied mechanical end anchorage with L-shaped angle and steel plate, respectively. The schematic of differences of each specimen is shown in Figure 4.

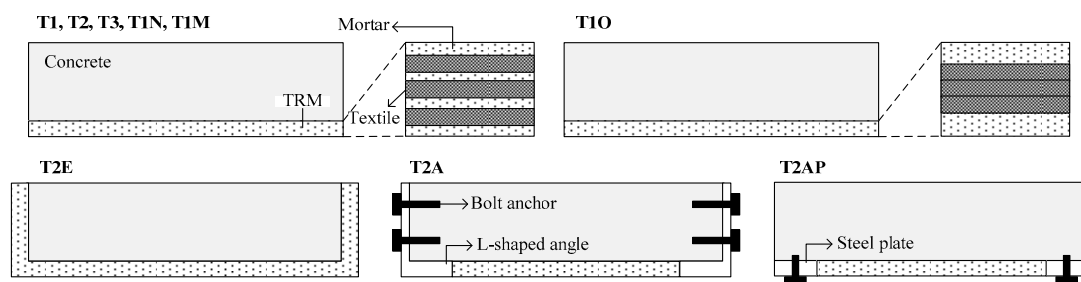


Figure 4. Schematic of TRM specimens.

2.4. Test Set-Up

The 4-point loading method with 3000 kN UTM was used at a rate of 0.1 mm/s under displacement control. As shown in Figure 2, the span of the specimen was 1300 mm, and the loading point was 400 mm in the mid-span. A linear variable differential transformer (LVDT) was installed at the mid-span to measure the deflection. Four concrete strain gauges and two steel strain gauges were installed at the mid-span. Extended PI gauge which consisted of two PI gauges with a 50 mm length and thin steel plate with a 300 mm length were attached at the mid-span of the TRM to measure the longitudinal deformation in the pure bending section.

3. Experimental Results and Discussion

3.1. Crack and Failure

Crack was observed with visual inspection. Similar flexural cracks appeared in all specimens as shown in Figure 5. The first cracks appeared in TRM at the pure bending section and developed towards both sides. After the occurrence of the crack of the TRM, crack of RC propagated at the same location where the TRM crack appeared. This is because the flexural stress was concentrated on the crack of the TRM and the concrete stress easily reached the tensile strength.

The number of cracks in RC was shown in Figure 6. The number of cracks in the pure bending section of the TRM specimen appeared more than that of control specimen. Therefore, TRM reinforcement appears beneficial for uniform distribution of cracks [17,20,25].

When the tensile force is applied to the textile and released in the matrix, the compressive force is applied to the matrix, and the initial crack strength of the TRM is increased as much as compressive stress. For a prestressed TRM, for the new crack to occur, the bond stress between textile and matrix must be increased as much as the sum of the initial compressive stress and tensile strength of the matrix. That is, the occurrence of a large crack is essential, and the number of cracks is decreased [20,26,27]. The textile of this study did not introduce enough force to cause sufficient elastic deformation of TRM. However, a slight tension of textile was maintained by applying mechanical anchors to T2A and T2AP. Therefore, it can be seen that the crack width and spacing was increased in the pure bending section as shown in Figure 6.

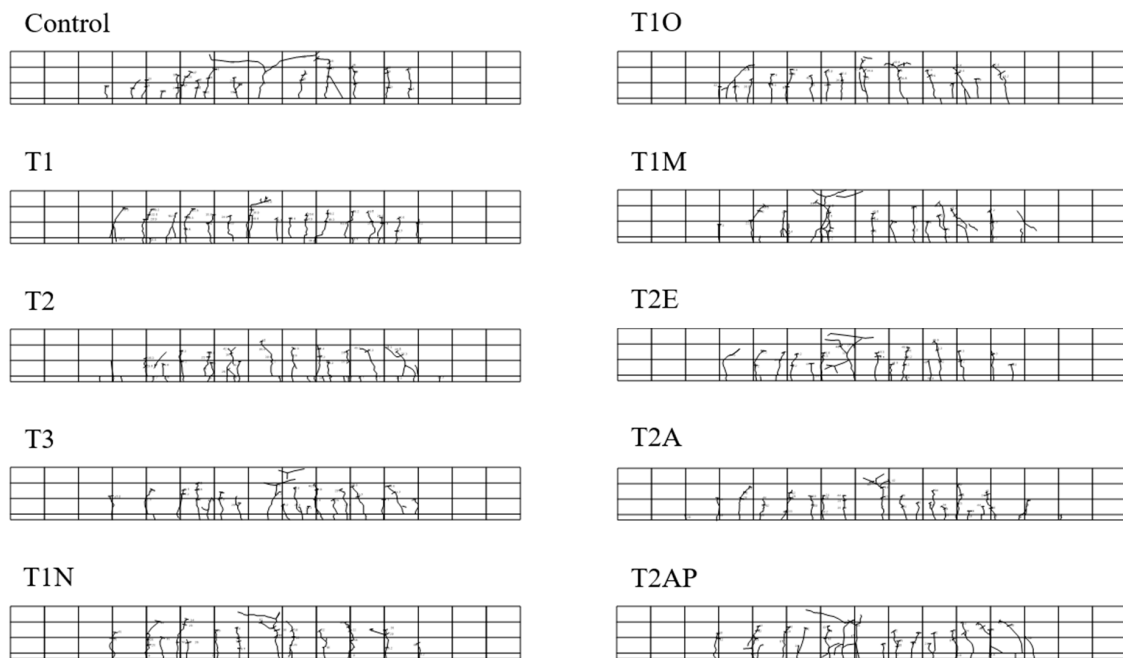


Figure 5. Crack patterns for all specimens at concrete crushing.

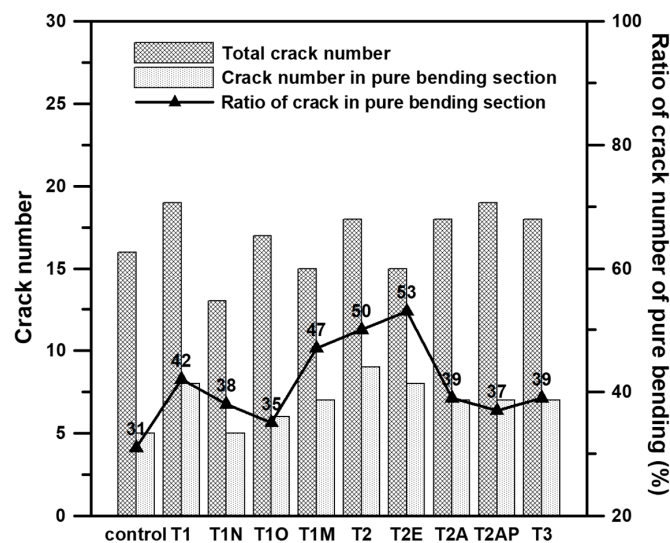


Figure 6. Crack number of all specimens.

The T1O applied one layer with lamination of three textile and T3 applied three layers with lamination of three textile. Thus, the bond area between textile and mortar of T1O and T3 was smaller than the other TRM specimens so that ratio of crack numbers of pure bending was low, as shown in Figure 6.

The failure modes of the TRM were shown as follows: (1) Textile rupture; (2) debonding between concrete substrate and TRM and textile rupture; and (3) textile slippage. After the failure of TRM, nearly the same plastic behavior of the control specimen was shown and, finally, crushing of concrete occurred. The failure modes of all specimens, listed in Table 6 and Figure 7, show three types of failure of the TRM. Figure 7a shows the textile rupture after the test of the T2AP. Figure 7b shows the debonding of the TRM strengthening layer of T2 after the ultimate load was reached. This debonding was also observed in T1O. Figure 7c shows the textile slippage of the T1M. The slippage of the textile occurred from yield load to crushing of concrete. After the end of the test, the textile had not failed, but showed crimp shape.

Table 6. Test results.

Name	Experiment Results					Failure Mode
	P_y (kN)	δ_y (mm)	P_u (kN)	δ_u (mm)	μ (δ_u/δ_y)	
RC	32.06	6.75	35.39	18.92	2.8	Concrete crushing
T1	33.66	7.48	-	-	-	Textile rupture
T1N	38.96	7.85	-	-	-	Textile rupture
T1O	38.22	8.18	39.21	10.79	1.32	Debonding and textile rupture
T1M	35.38	8.42	37.11	17.48	2.08	Textile slippage
T2	34.89	10.02	36.49	15.86	1.58	Debonding and textile rupture
T2E	40.69	8.85	42.29	12.45	1.41	Textile rupture
T2A	40.19	7.31	-	-	-	Textile rupture
T2AP	38.34	7.41	40.19	9.03	1.22	Textile rupture
T3	38.71	8.53	41.92	12.79	1.50	Textile rupture

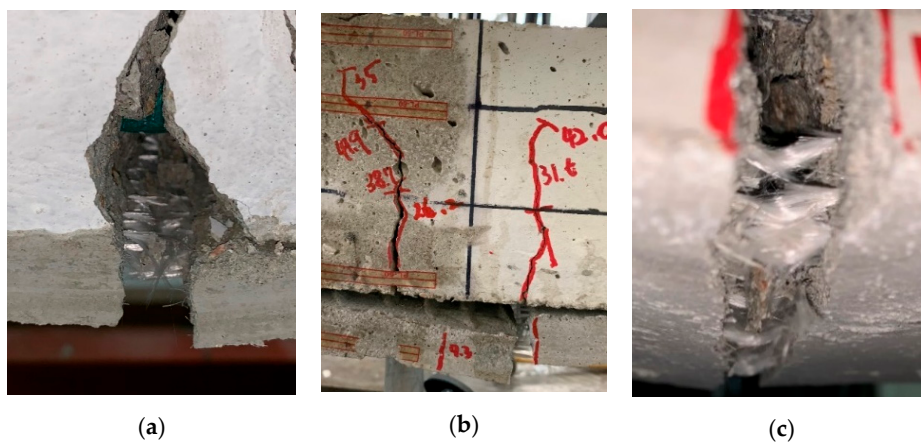


Figure 7. Failure modes of TRM: (a) Textile rupture of T2AP; (b) debonding and textile rupture of T2; (c) textile slippage of T1M.

3.2. Load and Deflection Relationship

The load and deflection curves for each comparison group are shown in Figures 8–10, and the results are listed in Table 6. The stiffness of TRM and control specimens were similar, except for T2, T2A, and T2AP. The decrease of the stiffness of the T2 was observed due to damage of the concrete beam during the grinding process. Increasing stiffness of T2A and T2AP was affected by applying a mechanical end anchorage.

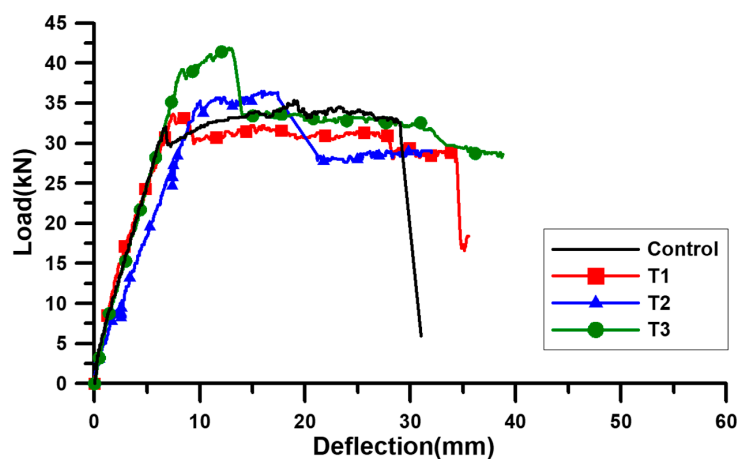


Figure 8. Load and deflection curve: Textile reinforced ratio.

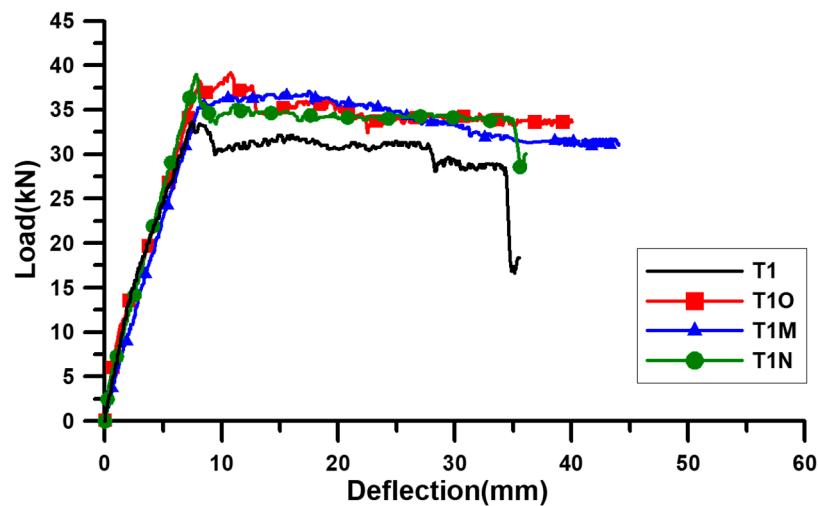


Figure 9. Load and deflection curve: Textile lamination and geometry.

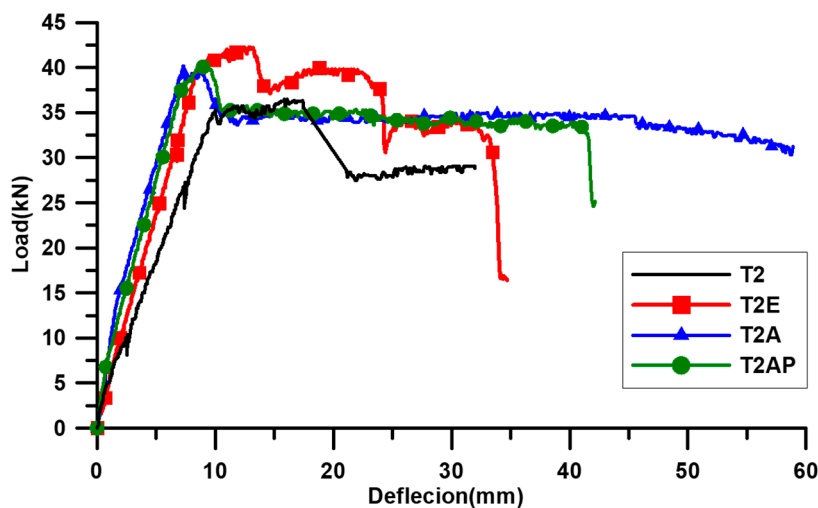


Figure 10. Load and deflection curve: End anchorage.

3.2.1. Textile Reinforcement Ratio

Figure 8 shows flexural behavior of the control, T1, T2, and T3 specimens according to the textile reinforcement ratio. The yield and ultimate loads of the control specimen were 32.06 kN and 35.39 kN, respectively. The yield load of T1 was 33.66 kN, which was 5% higher than that of the control specimen. As for T2, its yield and ultimate loads were 34.89 kN and 36.49 kN, respectively, which were 9% and 3% higher than that of the control specimen, respectively. For T3, its yield and ultimate loads were 38.71 kN and 41.92 kN, respectively, which were 21% and 18% higher than the control specimen, respectively. The strengthening effect of T1 and T2 was negligible because the ratio of increasing strength was less than 10%. In particular, the textile reinforcement ratio of T2 was twice that of T1, but the ratio of increase of the ultimate load was 3%.

Hegger et al. [28] reported that when the transversal action and the bending is applied to textile, the filament is damaged, and the load-bearing capacity is decreased. In addition, the bond performance of inner filaments is better, but inner filaments exhibit lower strain than outer filaments. To determine the complex behavior, inclined roving model in the crack was introduced, and the textile effectiveness was reduced about 50% for an angle of 45°. The load of T1 was decreased after the yielding of the steel rebar. T2 exhibited a yield load similar to T1 and showed a negligible increase in the ultimate load compared with the control specimen. This behavior of T1 and T2 indicates that the damage of the

non-impregnated textile in the crack increased with the increase of the load, and the strengthening efficiency decreased sharply.

The T3 showed sufficient improvement with higher ratio of increase of strength compared with T1 and T2. As shown in Table 6, T3 had similar load-bearing capacity of T2E, T2A, and T2AP with end anchor because there was enough textile to bear the load even if some of textile of the T3 was damaged. T2E, T2A, and T2AP were considered to be free of textile damage due to anchor. This is discussed in detail in Section 3.2.3. The higher the ratio of textile reinforcement, the more sufficient load-bearing capacity appears even if damage to the non-impregnated textile occurred.

3.2.2. Textile Lamination and Geometry

Figure 9 shows flexural behaviors of T1, T1N, T1O, and T1M according to textile lamination and geometry. The yield load of T1N was 38.96 kN, which was 16% higher than that of the T1 specimen. The yield load of T1O was 38.22 kN, which was 14% higher than that of T1. The ultimate load of T1O was 39.21 kN, which was a little higher than its yield load. T1O and T1N improved the load-bearing capacity with nearly the same increment. The textile of T1 was vulnerable to damage, as described in the previous section, Section 3.2.1. However, in case of T1O, because the textile applied at the same reinforcing axis by lamination, all filaments in the textile resist the loads acting on the TRM layer simultaneously, even if the inner filaments have a higher ratio in the total cross-section area of the textile. Therefore, T1O increased load-bearing capacity higher than that of T1. In the case of T1N with the process of pressing the mortar with a trowel after the application of the textile without fixing both ends of the textile, the spacing of the textile layer of T1N was decreased compared to that of T1, so that same effect of textile lamination of T1O was observed. However, unlike other specimens, the uncertainty in the fabrication process of non-stretching caused unstable behavior in which the load suddenly decreased due to the textile rupture at the yield load.

The yielding and ultimate load of T1M was 35.38 kN and 37.11 kN, respectively. The textile mesh size of T1M was changed from 8 mm to 24 mm. The yield load of T1M was 5% higher than that of T1, but the yield and ultimate load were decreased compared with T1N and T1O. Because the weft (transverse direction) roving of the textile applied to beams or one-way slabs is perpendicular to the longitudinal axis, there is no load-bearing capacity but it performs a mechanical interlock such as an anchor of warp (longitudinal direction) roving between interaction points [25]. Therefore, T1M had wider spacing of anchors that fix warp roving than other TRM specimens, so that the possibility of textile slippages increased, and load-bearing capacity decreased [16].

3.2.3. End Anchorage

Figure 10 shows flexural performances of T2, T2E, T2A, and T2AP according to the type of end anchorage. The yield and ultimate load of T2E were 40.69 kN and 42.29kN, respectively, which were 17% and 16% higher than that of T2, respectively. The yield load of T2A was 40.19 kN, which was 15% higher than that of T2. The yield and ultimate load of T2AP were 38.34 kN and 40.19kN, respectively, which were 10% higher than that of T2. In the case of T2E, the load dropped two times after the ultimate load, unlike other TRM specimens. The first load drop was caused by the rupture of the outer filaments due to increase in the stress in the crack. In general, the slippage of textile inside the matrix occurred if there was no clamping device with sufficient compressive force such as an anchor [25]. The textile of T2E was fixed to both ends of the beam, hence the inner filaments in the textile were fixed by anchor and the load was once again increased slightly. The slippage of inner filaments had occurred before the ultimate load was reached but was limited by bonding of the end anchorage until the second load drop occurred. Therefore, T2E improved the load-bearing capacity more than the non-end anchorage specimens but did not completely prevent slippage. The T2A and T2AP with bolt anchor prevented all slippage of the textile, and all the filaments of textile resisted the load simultaneously so that the stiffness and load-bearing capacity increased significantly.

3.2.4. Ductility

Figure 11 compares the ductility index, which is defined as the ultimate deflection, δ_u , divided by deflection at yield load, δ_y . The ductility of T1O, T1M, T2, T2E, T2AP, and T3 were 1.32, 2.08, 1.58, 1.41, 1.22 and 1.5, respectively. T1M showed higher ductility compared with other TRM specimens. Contrary to T1M, T2AP with mechanical end anchorage had the lowest ductility while suppressing slippage. The ductility of the control specimen was 2.8, and all TRM specimens were less ductile than that of the control specimen, and thus failed to ensure sufficient ductility for structural safety.

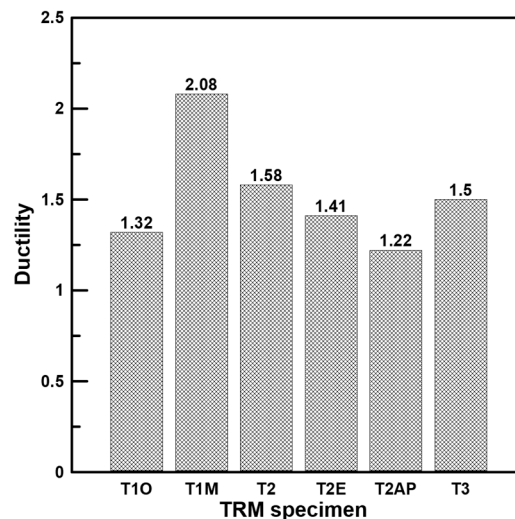


Figure 11. Comparison of ductility index of TRM specimen.

3.3. Strain

Strain changes according to height of specimen are shown in Figure 12. Strains of all specimens before yield were proportional to the distance from the neutral axis. As shown in Figure 12a, T1M clearly shows a sudden increase of TRM strain due to textile slippage between yield and ultimate load. As shown in Figure 12b, T3 shows the load was relatively proportional to the distance of the neutral axis until the ultimate load, although a significant change occurred from yield to ultimate load. Figure 12c shows a strain change of T2 at ultimate load and debonding of TRM. At this point, there is no proportional strain change along the neutral axis. In contrast, as shown in Figure 12d,e, T2AP and T2E showed proportional strain change of the TRM. T2AP had a constant strain variation until the ultimate load and perfectly prevented the slippage of textile. T2E showed almost the same behavior as the T3, but it can be seen that the strain variation was smaller than that of T3 by partially limited slippage of textile.

3.4. Comparison of Yield Loads of Studies Specimens

Experiment results showed that yield and ultimate load of TRM specimens were higher than those of the control specimen except T1, T1N, and T2A in ultimate load. The ratio of increase of yield load was especially higher than that of the ultimate load. After the yielding point of the TRM specimen, textile rupture occurred in T1, T1N, and T2A, and ductility of all specimens was lower than that of the control specimen. Therefore, considering the structural safety and serviceability, the strengthening effect of reinforced concrete with TRM using non-impregnated textile could be compared within yield load. Figure 13 shows yield load of all TRM specimens. Loads increased in proportion to the reinforcement ratio of T1, T2, and T3. The other specimens except T1M showed similar yield loads to that of the T3 specimen, which had the largest reinforcement ratio. Therefore, TRM strengthening using non-impregnated textiles could improve load-bearing capacity until yielding by using small mesh size, textile lamination, and fixing the textile with mechanical end anchorage.

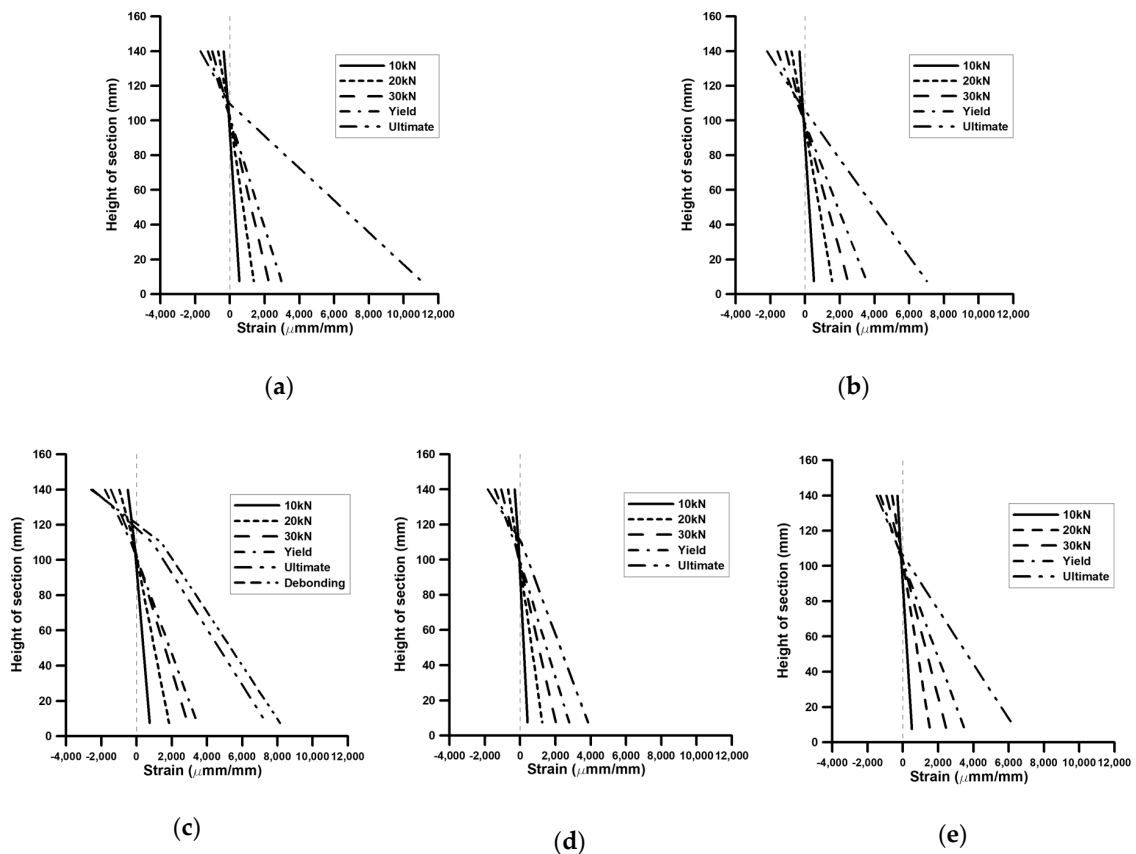


Figure 12. Strain distribution of different load levels: (a) T1M; (b) T3; (c) T2; (d) T2AP; (e) T2E.

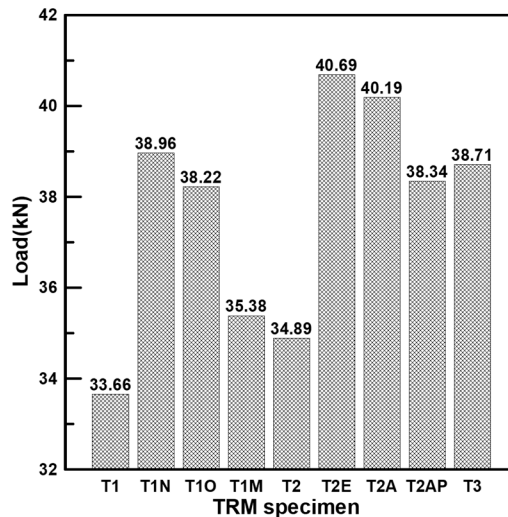


Figure 13. Comparison of yield loads of TRM specimen.

4. Conclusions

This study investigated the strengthening efficiency and flexural behavior of reinforced concrete (RC) beams strengthened by textile-reinforced mortar (TRM) with non-impregnated textile. For this purpose, the control specimen, an RC beam, was compared with nine TRM specimens.

1. There were multiple cracks in the pure bending of the TRM specimen compared with control specimen. However, in the case of using textile lamination, the ratio of bonding area with textile and mortar decreased compared to the total cross-sectional area of the textile, and in the case of

applying mechanical end anchorage (T2AP, T2A), the initial crack strength increased. In both cases, the cracking ratio of the pure bending section was lowered. Nevertheless, TRM strengthening was beneficial for uniform distribution of cracks.

2. Non-impregnated textile is easily damaged and slipped. Experimental results show that the case of lamination of textile can reduce the damage of the textile, but it does not prevent slippage. In the case of applying mechanical end anchorage, the slippage of the textile was expected to be completely prevented.
3. Considering the low ductility of all TRM specimens compared with control specimens and that no ultimate load was observed in some specimens, the behavior of TRM specimens after yield load was considered to be unstable. Therefore, the TRM strengthening effect of non-impregnated textiles could be compared with the behavior before the yield load considering structural safety and serviceability.
4. TRM strengthening using non-impregnated textiles increased the efficiency as the textile reinforcement ratio and textile lamination increased and the mesh size of the textile decreased and mechanical end anchorage applied. In this study, it was possible to have a load-bearing capacity similar to T3 with the largest textile reinforcement ratio by applying the above method.

Note that the conclusion is based on the experimental results. To generalize experimental results, a more experimental and analytical study is needed.

Author Contributions: Investigation, methodology, and writing—original draft, J.P.; writing—review and editing, S.H.; project administration and supervision, S.-K.P.

Funding: This research was funded by National Research Foundation of Korea, grant number NRF-2017R1A2B2012535.

Acknowledgments: This work was supported by the National Research Foundation of Korea (NRF) grant funded by the Korea government (MSIP) (No. NRF-2017R1A2B2012535) and by the Basic Science Research Program through the National Research Foundation of Korea (NRF) and funded by the Ministry of Education (2016R1A6A3A11931804).

Conflicts of Interest: The authors declare no conflict of interest.

References

1. American Society of Civil Engineers. *2017 Infrastructure Report Card*, 1st ed.; American Society of Civil Engineers: Reston, VA, USA, 2017; pp. 7–8.
2. Koutas, L.N.; Bournas, D.A. Flexural Strengthening of Two-Way RC Slabs with Textile-Reinforced Mortar: Experimental Investigation and Design Equations. *J. Compos. Constr.* **2017**, *21*, 1–11. [[CrossRef](#)]
3. Arduini, M.; Nanni, A. Behavior of Precracked RC Beams Strengthened with Carbon FRP Sheets. *J. Compos. Constr.* **1997**, *1*, 63–70. [[CrossRef](#)]
4. Hong, S.; Park, S.K. Effect of prestress levels on flexural and debonding behavior of reinforced concrete beams strengthened with prestressed carbon fiber reinforced polymer plates. *J. Compos. Mater.* **2013**, *47*, 2097–2111. [[CrossRef](#)]
5. Hong, S.; Park, S.K. Prestressing effects on the performance of concrete beams with near-surface-mounted carbon-fiber-reinforced polymer bars. *Mech. Compos. Mater.* **2016**, *52*, 305–316. [[CrossRef](#)]
6. Bramshuber, W. *Textile Reinforced Concrete—State of the Art Report of RILEM TC 201-TRC*, 1st ed.; RILEM: Aachen, Germany, 2006; pp. 1–271.
7. Babaeidarabad, S.; Loreto, G.; Nanni, A. Flexural Strengthening of RC Beams with an Externally Bonded Fabric-Reinforced Cementitious Matrix. *J. Compos. Constr.* **2014**, *18*, 1–11. [[CrossRef](#)]
8. Baiee, A.; Rafiq, I.; Lampropoulos, A. Innovative technique of textile reinforced mortar (TRM) for flexural strengthening of reinforced concrete (RC) beams. In Proceedings of the 2nd International Conference on Structural Safety Under Fire and Blast Loading, London, UK, 10–12 September 2017.
9. Hartig, J.; Häußler-Combe, U.; Schicktan, K. Influence of bond properties on the tensile behaviour of Textile Reinforced Concrete. *Cem. Concr. Compos.* **2008**, *30*, 898–906. [[CrossRef](#)]

10. Colombo, I.G.; Magri, A.; Zani, G.; Colombo, M.; di Prisco, M. Textile Reinforced Concrete: Experimental investigation on design parameters. *Mater. Struct.* **2013**, *46*, 1933–1951. [[CrossRef](#)]
11. Banholzer, B.; Brockmann, T.; Brameshuber, W. Material and bonding characteristics for dimensioning and modelling of textile reinforced concrete (TRC) elements. *Mater. Struct.* **2006**, *39*, 749–763. [[CrossRef](#)]
12. Williams Portal, N.; Lundgren, K.; Walter, A.M.; Frederiksen, J.O.; Thrane, L.N. Numerical modelling of textile reinforced concrete. In Proceedings of the 8th International Conference on Fracture Mechanics of Concrete and Concrete Structures, FraMCoS 2013, Toledo, Spain, 11–14 March 2013; pp. 886–897.
13. Zastrau, B.; Richter, M.; Lepenies, I. On the Analytical Solution of Pullout Phenomena in Textile Reinforced Concrete. *J. Eng. Mater. Technol.* **2003**, *125*, 38–43. [[CrossRef](#)]
14. Iorfida, A.; Verre, S.; Candamano, S.; Ombres, L. Tensile and Direct Shear Responses of Basalt-Fibre Reinforced Mortar Based Materials. In Proceedings of the Strain-Hardening Cement-Based Composites (SHCC4), Deresden, Germany, 18–20 September 2017; RILEM: Aachen, Germany, 2018; pp. 544–552.
15. Papanicolaou, C.G.; Papantoniou, I.C. Mechanical Behavior of Textile Reinforced Concrete (TRC) / Concrete Composite Elements. *J. Adv. Concr. Technol.* **2010**, *8*, 35–47. [[CrossRef](#)]
16. Yin, S.P.; Xu, S.L. An Experimental Study on Improved Mechanical Behavior of Textile-Reinforced Concrete. *Adv. Mater. Res.* **2011**, *168–170*, 1850–1853. [[CrossRef](#)]
17. Yin, S.; Xu, S.; Lv, H. Flexural Behavior of Reinforced Concrete Beams with TRC Tension Zone Cover. *J. Mater. Civ. Eng.* **2014**, *26*, 320–330. [[CrossRef](#)]
18. Yin, S.P.; Xu, S.L.; Wang, F. Investigation on the flexural behavior of concrete members reinforced with epoxy resin-impregnated textiles. *Mater. Struct.* **2015**, *48*, 153–166. [[CrossRef](#)]
19. Kamani, R.; Kamali Dolatabadi, M.; Jeddi, A.A.A. Flexural design of textile-reinforced concrete (TRC) using warp-knitted fabric with improving fiber performance index (FPI). *J. Text. Inst.* **2017**, *109*, 492–500. [[CrossRef](#)]
20. Liu, L.; Du, Y.; Zhou, F.; Pan, W.; Zhang, X.; Zhu, D. Flexural Behaviour of Carbon Textile-Reinforced Concrete with Prestress and Steel Fibres. *Polymers* **2018**, *10*, 98.
21. Raoof, S.M.; Koutas, L.N.; Bournas, D.A. Textile-reinforced mortar (TRM) versus fibre-reinforced polymers (FRP) in flexural strengthening of RC beams. *Constr. Build. Mater.* **2017**, *151*, 279–291. [[CrossRef](#)]
22. Jesse, F.; Weiland, S.; Curbach, M. Flexural strengthening of RC structures with textile-reinforced concrete. *ACI Spec. Publ.* **2008**, *250*, 49–58.
23. Gutierrez, E.; Bono, F. *Review of Industrial Manufacturing Capacity for Fibre-Reinforced Polymers as Prospective Structural Components in Shipping Containers*; Publications Office of the European Union: Luxembourg, 2013; pp. 5–12.
24. Peled, A. Pre-tensioning of fabrics in cement-based composites. *Cem. Concr. Res.* **2007**, *37*, 805–813. [[CrossRef](#)]
25. Koutas, L.N.; Tetta, Z.; Bournas, D.A.; Triantafillou, T.C. Strengthening of Concrete Structures with Textile Reinforced Mortars: State-of-the-Art Review. *J. Compos. Constr.* **2019**, *23*, 1–20. [[CrossRef](#)]
26. Reinhardt, H.W.; Krüger, M.; Große, C.U. Concrete Prestressed with Textile Fabric. *J. Adv. Concr. Technol.* **2003**, *1*, 231–239. [[CrossRef](#)]
27. Du, Y.; Zhang, M.; Zhou, F.; Zhu, D. Experimental study on basalt textile reinforced concrete under uniaxial tensile loading Experimental study on basalt textile reinforced concrete under uniaxial tensile loading. *Constr. Build. Mater.* **2017**, *138*, 88–100. [[CrossRef](#)]
28. Hegger, J.; Will, N.; Bruckermann, O.; Voss, S. Load-bearing behaviour and simulation of textile reinforced concrete. *Mater. Struct.* **2006**, *39*, 765–776. [[CrossRef](#)]

